COMPDYN 2013
4th ECCOMAS Thematic Conference on
Computational Methods in Structural Dynamics and Earthquake Engineering
M. Papadrakakis, V. Papadopoulos, V. Plevris (eds.)
Kos Island, Greece, 12–14 June 2013

QUANTIFICATION OF RESIDUAL AXIAL CAPACITY OF BEAM-COLUMN JOINTS IN EXISTING CONCRETE BUILDINGS UNDER SEISMIC LOAD REVERSALS

Wael M. Hassan[1] **and Jack P. Moehle**[2]

[1] American University in Cairo
New Cairo, Egypt
waelhassan@aucegypt.edu

[2] University of California, Berkeley
Berkeley, CA, USA
moehle@berkeley.edu

Keywords: Beam-Column Joint, Axial Capacity, Seismic, Concrete, Existing Buildings.

Abstract. *Earthquake reconnaissance has reported the substantial damage that can result from inadequate beam-column joints in earthquake shaking. In some cases, failure of older-type corner joints appears to have led to building collapse. Insignificant research attention has been focused on beam-column joints of older construction that may be seismically vulnerable. Concrete buildings constructed prior to developing details for ductility in the 1970s normally lack joint transverse reinforcement (unconfined joints). The available literature concerning the performance of such joints is relatively limited, but concerns about their seismic axial failure exist. The main goal of this study is to quantify the axial collapse vulnerability of shear-damaged unconfined exterior and corner beam-column joints under cyclic load reversals. The quantification of the residual axial capacity of these joints is performed incorporating the test results of four full-scale three dimensional corner beam-column joint sub-assemblages, along with few other tests available in the literature to develop analytical models for joint axial capacity. Two axial capacity models designed for unconfined joints were developed. The proposed models correlated with previous test results. Within the practical range of beam-column joint dimensions, the axial failure appears unlikely. However, this result is obtained based on a small dataset. More tests are needed to verify the developed models and to investigate the axial failure likelihood for joint dimensions not included in the presented models.*

1 INTRODUCTION

Very few unconfined joint tests are available with confirmed axial failure. Unfortunately during laboratory joint tests, a common practice has been to terminate the test after dropping to 80% of lateral load resistance without testing the axial capacity of the joint. However, many post-earthquake reconnaissance studies report building damage or collapse that might be attributed to exterior and corner beam-column joint failures. No interior joint axial failures have been identified. An important aspect of the assessment of an existing building is to assess drift capacity after the onset of shear failure until reaching axial failure. Shear failure of joints and columns in older buildings can occur at relatively low drifts. Whether the axial failure of a shear damaged joint will precede the axial failure of a shear damaged column leading to a progressive collapse is not certain. The axial capacity of shear damaged columns and joints should be input as limit states in building simulation models, such as the macro model presented in Hassan and Moehle [9], to realistically represent the ignition of progressive collapse. From an economic viewpoint, if a joint can reliably support gravity load after its lateral strength degradation begins, it may be possible to achieve considerable savings by considering this particular joint as a secondary component.

2 MODES AND MECHANISMS OF JOINT AXIAL FAILURE

Different approaches were used to decide the point of joint axial failure during previous joint tests. Since most tests were performed under constant axial load, a common sign of joint axial failure was a significant drop in axial load even without full disintegration of the joint. This approach could be sometimes misleading since the axial load may decrease for several reasons including axial stiffness degradation because of cracking, or hydraulic pressure drop for a mechanical reason. A better indicative sign of axial failure is the axial shortening below a threshold limit. Axial failure in most of the joints tested in Hassan [7] seemed indicated for an axial joint strain of about 0.005 to 0.006. The third approach of confirming axial failure is the total collapse of the specimen by dynamic instability due to reaching joint axial capacity.

Different modes of joint axial failure were observed during previous tests and following past earthquakes. Figure 1 shows joint damage interpreted as axial failure during past earthquakes and joint tests. For the past earthquake axial failures, whether the joint axial failure occurred first, triggering partial or total collapse, or the joint axial failure was a consequence of column axial failure is unknown.

Figure 2 displays the axial failure modes of specimens U-J-1, U-J-2, U-BJ-1 and B-J-1 of Hassan [7]. In specimen U-J-1, the starting gravity load ratio was 0.21. The axial load ratio at peak joint shear strength was 0.31 while that at axial failure was 0.20. The drift ratio capacity at axial failure was relatively high (9.68%). The joint core was severely damaged prior to reaching axial failure. During axial failure, a sliding failure on the diagonal shear failure plane occurred. As can be seen in Fig. 2, the failure mode of the column longitudinal reinforcement is a “side-sway” mode rather than a “buckling” mode.

Figure 2.c shows the failure mode of specimen U-J-2 whose axial load ratio at peak joint shear strength was 0.44 while that at axial failure was 0.41. The drift capacity at axial failure was 3.06%, with a maximum drift ratio 3.42% before axial failure. A buckling failure mode of column reinforcing bars is obvious. A sliding failure on the diagonal shear failure surface was observed following removal of damaged concrete debris, although it was less apparent than that in specimen U-J-1. Similar axial failure modes to that of specimen U-J-2 were observed in specimens B-J-1 and U-BJ-1.

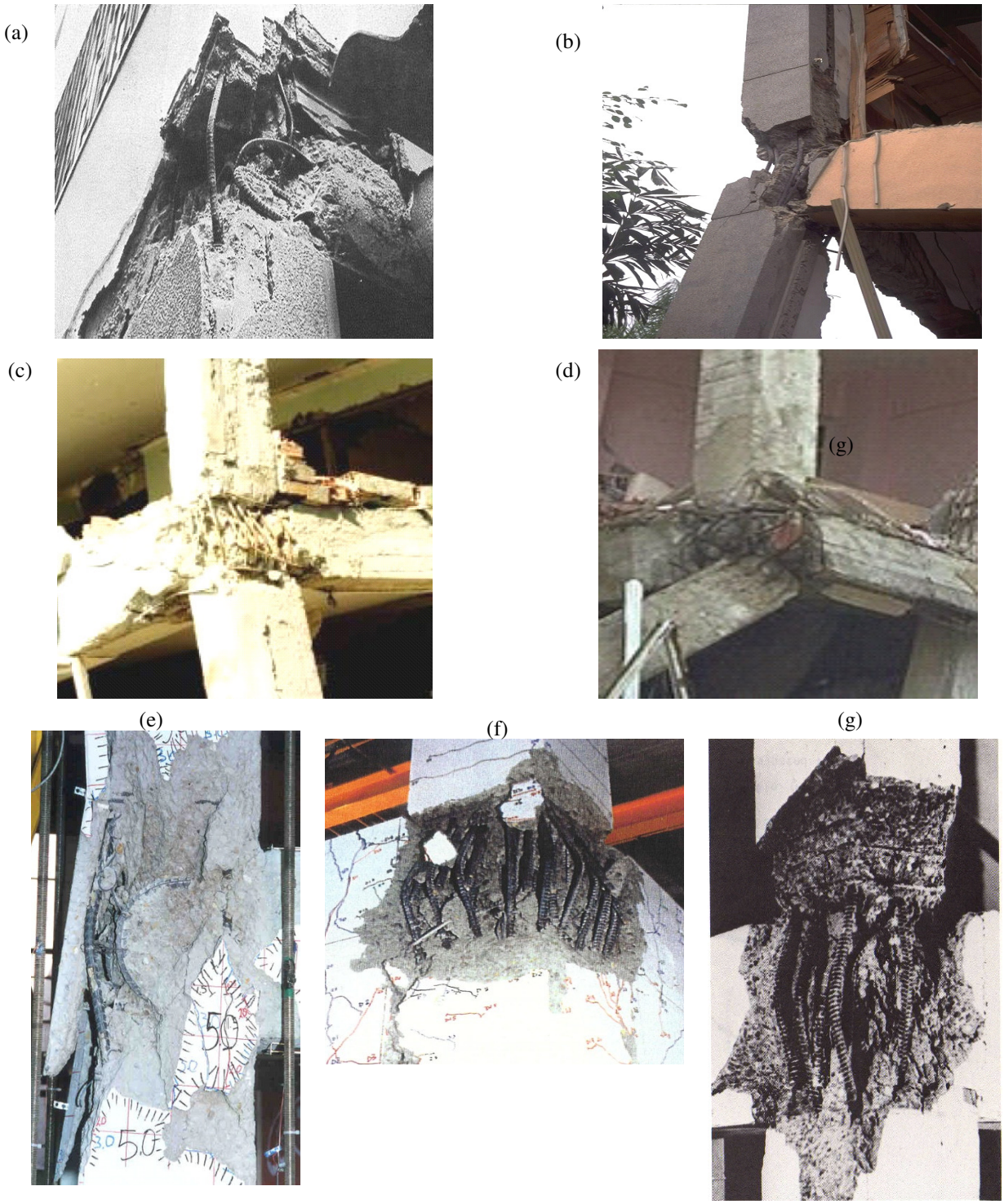

Figure 1 Joint axial failure during past earthquakes and laboratory tests: Caracas, Venezuela earthquake, Pagni [14], (b) Taiwan Chi-Chi 1999 earthquake, NISEE [13], (c) Izmit, Turkey earthquake of 1999, Engindeniz [4], (d) Izmit, Turkey earthquake of 1999, NISEE [13], (e) Exterior joint test, Pantelides et al. [15], (f) Corner joint test, Priestley and Hart [17], (g) Corner simulated joint test, Uzumeri [19]

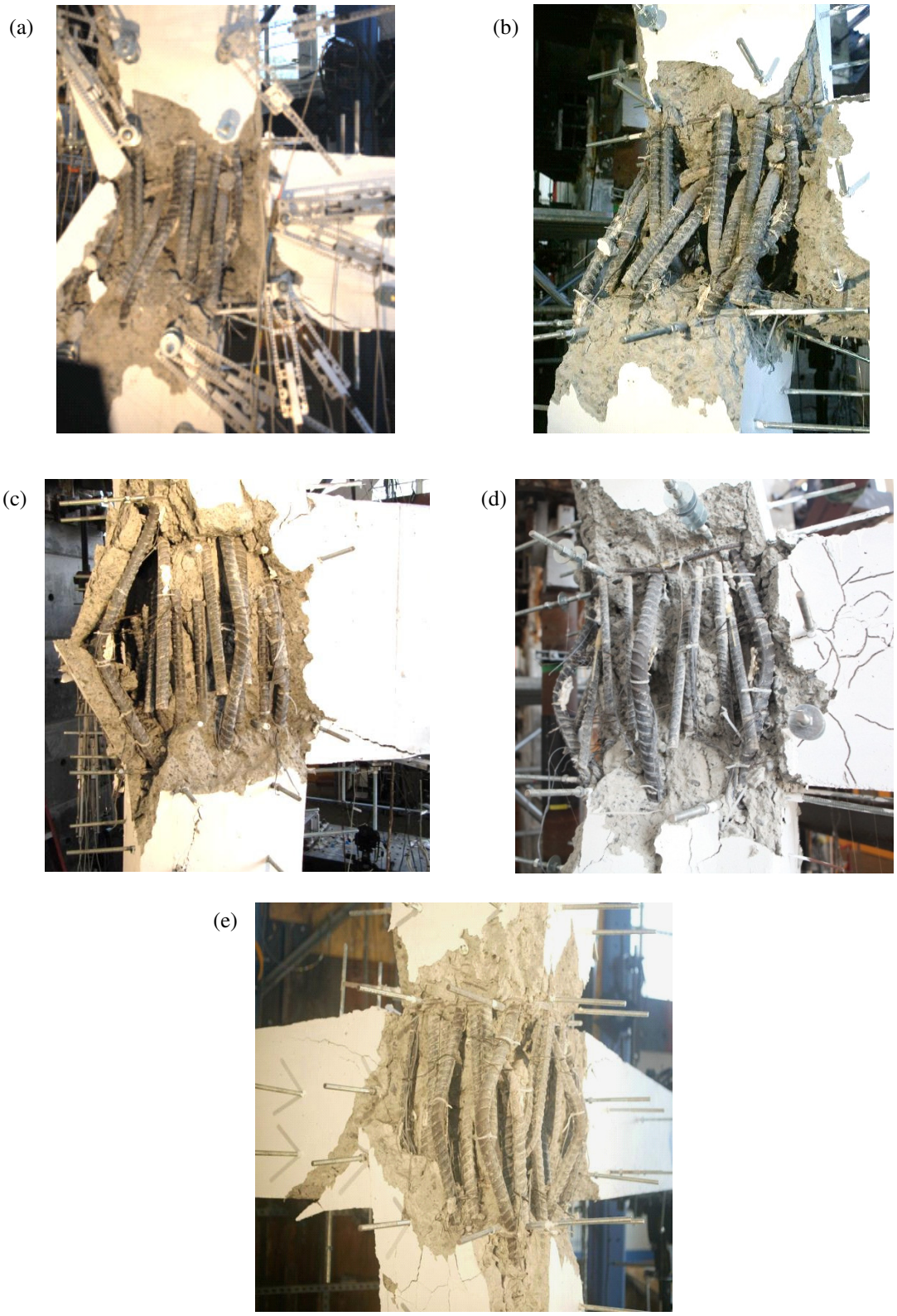

Figure 2 (a), (b) Column bar "side-sway" axial failure mode in specimen U-J-1, (c) Bar buckling axial failure mode in specimen U-J-2, (d) specimen U-BJ-1, and (e) specimen B-J-1, Hassan [7]

The different failure modes observed for the different test specimens are believed to be due to the different levels of axial loads in the tests. The "sliding" axial failure on the previously damaged shear failure plane in the joint suggests that the classical shear friction theory can be used to explain the failure mechanism. Elwood and Moehle [3] presented a derivation for an axial capacity model for shear-damaged columns based on the interaction between shear-friction surface and axial capacity of column longitudinal reinforcement.

As described in Elwood and Moehle [3], axial failure of a shear-damaged column can occur by sliding along an inclined crack plane, with resistance provided by transverse reinforcement clamping the crack and longitudinal reinforcement supporting axial force directly. Axial failure of a joint may be viewed similarly. After developing joint shear failure, the axial load will be supported by shear friction on the diagonal shear failure plane and the axial capacity of column reinforcing bars. Whether these two mechanisms work concurrently is dependent on the location of column bar within the joint. The share of each column bar of the axial load at the joint region might not be equal. However, for simplification purpose, it will be generally assumed that all column bars will share equally a small portion of axial load in the shear-damaged joint.

3 OBSERVED AXIAL CAPACITY OF BEAM-COLUMN JOINTS

As mentioned earlier, few previous joint tests were continued until reaching axial failure. For exterior unconfined joint tests, four such test specimens were reported by Pantelides et al. [14]. In this group of tests called Unit 3, Unit 4, Unit 5, and Unit 6, axial failure was identified by a drop in the constant axial load applied to the column. Priestley and Hart [16] report axial failure of an unconfined corner joint. Axial failure of this corner joint, denoted "As built", was identified by crushing of joint core along with buckling of column bars in the joint and eventually loss of axial carrying capacity. In addition, one corner simulated joint, SP5, with a pre-cracked transverse stub experienced axial failure in tests performed by Uzumeri [19]. All four unconfined corner joints tested in Hassan [7] (denoted NEES Joints) experienced axial failure as described in a previous section.

Figure 3 plots the relationship between axial failure load and the maximum drift reached prior to axial failure for the ten joints mentioned above. In addition, a database of 37 previous exterior and corner joint tests in which axial failure was not reached also is included. The axial load ratio and drift ratio for this database reflect the test termination values. This database includes joints tested by Wong [20], Park [16], Hwang et al. [11], Karayannis et al. [12], Clyde et al. [2], Uzumeri [19], Tsonos [18], Hanson and Conner [5] and [6] and Antonopoulos and Triantafillou [1]. The size of axial failure joints database is relatively small compared to that of non-axial failure joints. However, several useful observations can be made from this plot:

1. It appears that exterior and corner joints may be susceptible to axial failure under very large drifts or under high axial loads.
2. A general trend of a decreased axial failure drift capacity is associated with higher axial loads except for joint U-BJ-1, which will be discussed later.
3. Excluding joint U-BJ-1, an inverse proportionality between axial failure load and drift ratio can be observed.
4. The proportionality between axial failure load and drift ratio for the NEES J-Failure joints is offset from that between previous joint tests with axial failure. J-Failure mode is defined as the joint shear failure without beam or column yielding. Some differences exist between NEES J-Failure joints and other tests. The NEES tests include a

slab whereas others did not, and relatively fewer cycles were included than were included for some of the other tests.

5. Based on previous joint tests that did not experience axial failure, an axial failure safe zone can be drawn as shown in Fig. 3. Inclined line A defines a fairly clear demarcation between tests with and without axial failure. Line B is more tenuous, as it extends to high axial load levels for which few tests are available. The inclined line A can be algebraically expressed as

$$\left(\frac{\Delta}{L}\right) \leq \frac{1}{9} - \frac{P}{2.72 f_c^{'} A_g}$$

6. One test shown in Fig. 3 is the first unconfined joint test reported by Hanson and Conner (Specimen V) [5]. In this test, an unrealistically constant high axial load ratio of 0.95 was used. In spite of the substantial axial load, the specimen was able to survive 5.2% drift without axial failure. The somewhat peculiar combination of high axial load and high drift ratio could not be explained.
7. Specimen U-BJ-1 also stands apart from the trend of the other data. The reason for this is that the drift ratio is not the best marker of joint deformation capacity in this specimen, since most of the drift was contributed by significant beam yielding before shear failure (BJ-Failure mode), with joint axial failure delayed until very late stages of loading. Specimen 7 tested by Hanson and Conner [5] showed similar behavior. It was loaded under 0.50 constant axial load ratio and experienced a BJ-shear failure mode, with a substantial yielding and deformation of the beam. Under this high axial load, the specimen was able to survive a 5.1% drift ratio without axial failure. This result is also off the trend shown in Fig. 3 and suggests a much more relaxed axial failure drift capacity for specimens failing in shear by BJ failure mode under very high axial load. It is then likely that joints with BJ-Failure mode under high axial load ratio (more than 0.30) will survive drift ratios much larger than their J-Failure counterparts.
8. It is surprising that joint SP5, with 0.51 axial load ratio, experienced a BJ-Failure mode at 1.6% drift and axial failure at 3.5% drift only, unlike specimens U-BJ-1 and Specimen 7 mentioned above. This might be attributed to the arbitrary loading history used by Uzumeri [19] that decided number of cycles and displacement amplitudes during the test based on the observed behavior.

Figures 4 and 5 compare drifts at shear failure and drifts at axial failure for joints sustaining axial failures. The vertical axis plots the axial load at axial failure. Joints with higher axial load tended to sustain axial failure sooner after shear failure than did joints with lower axial loads, although the trend is not strong and there are exceptional cases. Specimen U-BJ-1 is one of the exceptions, for the reason explained earlier. It is highly informative to observe that a minimum μ_f of 2 seems a lower bound for drift ratio at axial failure to that at shear failure.

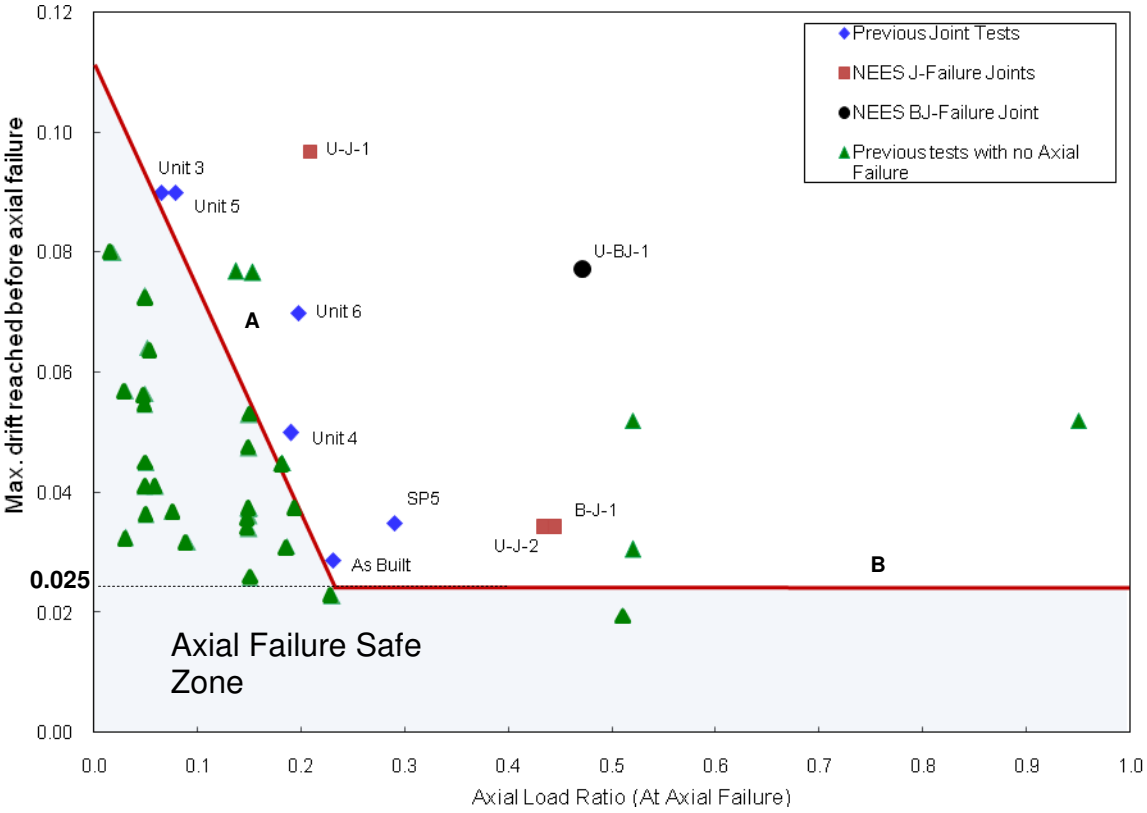

Figure 3 Axial load-drift ratio relationship at axial failure (or test termination) for exterior and corner joints

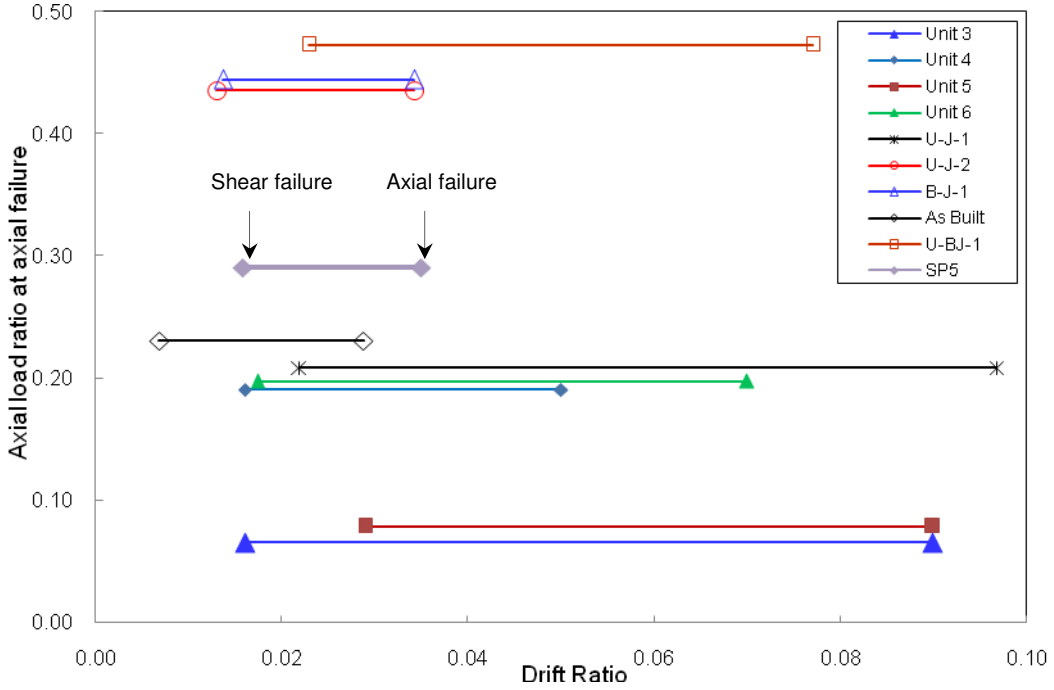

Figure 4 Relation between axial load at axial failure and drift ratio

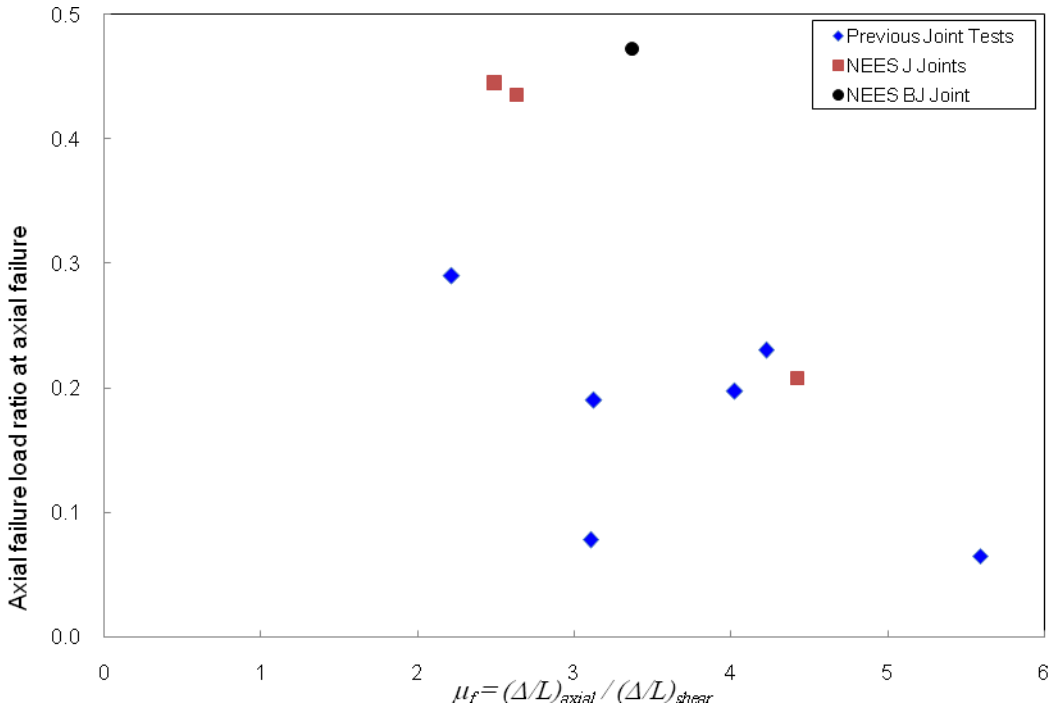

Figure 5 Relation between axial load at axial failure and drift at shear failure and at axial failure.

4 PROPOSED AXIAL CAPACITY MODELS FOR UNCONFINED JOINTS

4.1 Background

Based on Elwood and Moehle [3] axial capacity model for columns, an analogous model for application to unconfined joints is proposed. The model is based on observation of axial failure modes. The model assumes that the primary failure mechanism is along a shear friction surface of the previously shear-damaged joint, with column longitudinal reinforcement acting in axial load providing a secondary mechanism triggered after shear-friction failure on the shear failure plane. This section presents two axial capacity models for unconfined beam-column joints. These models are intended to be used with joints experiencing J-shear failure mode with any axial load level and BJ-failure mode with axial load ratio below 0.3. As discussed in a previous section, the axial failure of a BJ shear failure controlled joint under high axial load is not likely until very large drifts.

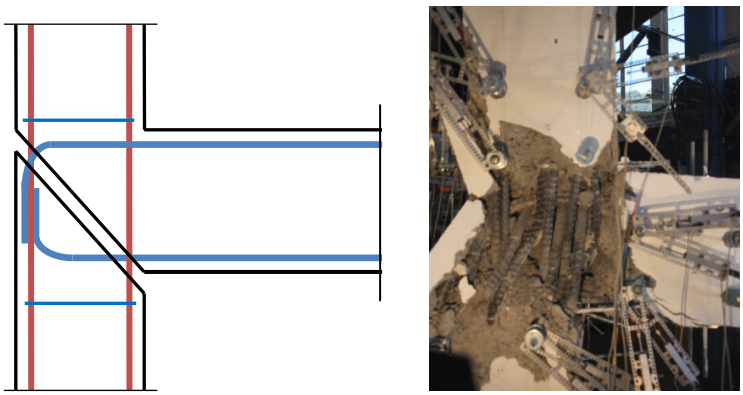

Figure 6 Development of shear-friction model for joint axial capacity based on experimental observation, (a) Proposed sliding mechanism, (b) Observed damage after axial failure, specimen U-J-1

4.2 Model 1: Analytical Shear-Friction Capacity Model

After joint shear failure along the major diagonal crack corresponding to the inclination of the main diagonal concrete joint strut, shear resistance starts to degrade. In many cases, however, the axial load at peak displacement does not immediately drop as discussed Hassan and Moehle [8]. Substantial axial load from the upper column must be transferred across the joint shear failure surface. Experimental observation of joint axial failure suggests transferring this axial load by shear-friction across the shear failure plane. Several shear-friction models are available; however, the classical shear-friction model adopted by ACI 318-08 and used by Elwood and Moehle [3] for shear-critical columns is used here.

Figure 7 shows the free body diagram of the upper block of the beam-column joint sub assemblage after shear failure. The critical crack angle θ can be calculated using the strut-and-tie model developed in Hassan, et al. [10] for joint shear strength. The axial failure is evident to take place during the downward loading of beam. Some simplifying assumptions are made next.

V_b and V_j are the beam shear force and joint shear force at join shear failure, respectively. Since the beam shear force $V_{b,a}$ and joint shear force $V_{j,a}$ at axial failure are not always insignificant like the case of columns (Elwood and Moehle [3]), they cannot be neglected in formulating the equilibrium equations. The dowel action provided by the longitudinal column and beam reinforcement will be implicitly included in the shear friction resistance $V_{sf;}$ hence they will not appear in the equilibrium equations. The total axial capacity of column reinforcement bars is denoted ΣP_s. The beam longitudinal reinforcement will act as shear-friction reinforcement holding the lower concrete block (the column) from separation. At the axial failure, the force in both top and bottom longitudinal beam bars will be tensile within the joint regardless the sense of the force within beam span.

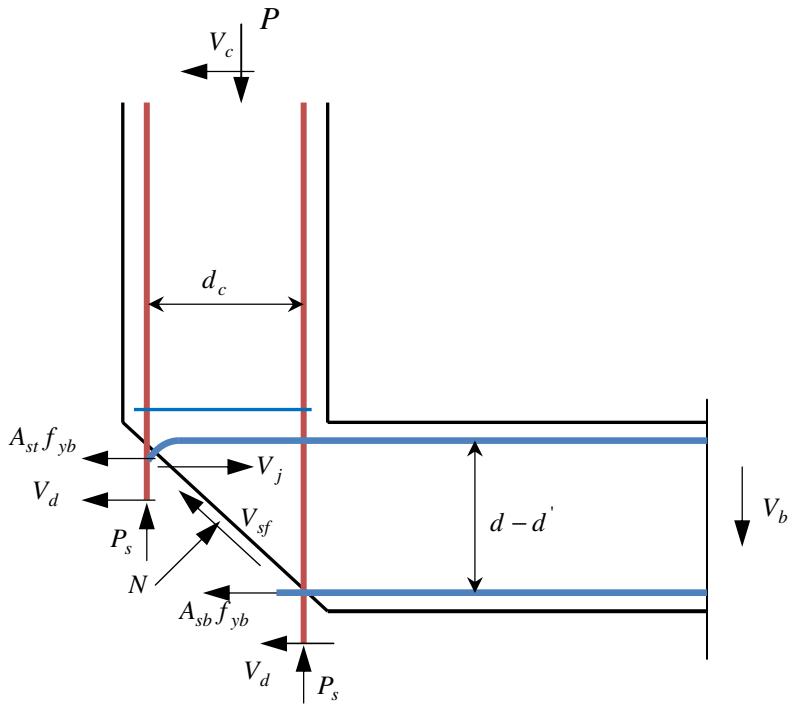

Figure 7 Free body diagram for beam-column joint at the onset of axial failure

The top beam longitudinal reinforcement appears to be less efficient in resisting shear friction since it experiences bond failure at earlier stage. More importantly, the portion of the

top beam bars holding the lower concrete block is usually the hook tail which is very poorly embedded and bonded to concrete at late stages of loading because of cover spalling or detachment. Accordingly, the resistance of top beam bars will not be included in the equilibrium equations. Based on the abovementioned simplifying assumptions, the equilibrium equations in the horizontal and vertical directions can be respectively written as:

$$N\sin\theta + V_j = V_{sf}\cos\theta + A_{sb}f_{yb} + \Sigma V_d \tag{1}$$

$$P + V_b = N\cos\theta + V_{sf}\sin\theta + \Sigma P_s \tag{2}$$

The proposed model assumes that joint axial capacity is primarily dependent on shear-friction mechanism. Column longitudinal axial capacity is considered secondary to shear-friction mechanism, which is triggered only after shear-friction failure. The calculation of axial capacity of column bars presented in Hassan [7] shows that this capacity is relatively small. Even if a portion of axial load is supported by column bars immediately before axial failure, suggesting a concurrent collective mechanism, this portion is insignificant as suggested by Elwood and Moehle [3]. Accordingly, this quantity will not be included in the model. Only the final model equations are presented herein for brevity. The model derivation is thoroughly presented in Hassan [7]. The model relates the axial load P to the drift capacity at axial failure $(\Delta/L)_{axial}$. It can also be used reversely to find the axial load capacity for a given drift ratio. More test data regarding axial failure of exterior and corner beam column joints is needed to refine and validate the expressions for lateral load capacity at axial failure.

$$\left(\frac{\Delta}{L}\right)_{axial} = 0.031\left\{\frac{(P+V_{b,a})\tan\theta + (V_{j,a} - A_{sb}f_{yb})}{(P+V_{b,a}) - (V_{j,a} - A_{sb}f_{yb})\tan\theta}\right\}^{-0.25} \tag{3}$$

$$\left(\frac{\Delta}{L}\right)_{axial} = 0.031\left\{\frac{(P+\chi\chi_a V_j)\tan\theta + (\chi_a V_j - A_{sb}f_{yb})}{(P+\chi\chi_a V_j) - (\chi_a V_j - A_{sb}f_{yb})\tan\theta}\right\}^{-0.25} \tag{4}$$

$$V_{j,a} = \left(1.1\frac{P}{f_c^{'}A_j} - 0.03\right).V_j = \chi_a V_j \tag{5}$$

$$V_{b,a} = \left(1.1\frac{P}{f_c^{'}A_j} - 0.03\right).V_b = \chi_a V_b \tag{6}$$

$$V_b = \frac{1}{\frac{L - h_c/2}{jd_b} - \frac{L}{H}} = \chi V_j \tag{7}$$

where: L is half the beam span, H is floor height, h_c is column depth, j=0.9, and d_b is the effective beam depth.

4.3 Empirical Shear-Friction Capacity Model

The above theoretically based shear-friction model is plausible if enough knowledge on the residual joint shear capacity at axial failure can be confirmed. It also contains two

empirical components, namely the estimation of effective shear-friction coefficient and the residual shear capacity at axial failure. The model is delivered finally in a rather lengthy expression. These factors motivated investigating the possibility of the presence of a trend between drift ratio and the axial failure load normalized by the influential parameters of the shear-friction phenomenon. The goal of this attempt was to develop a simpler empirical expression for quick estimation of drift capacity at axial failure eliminating the need for residual joint shear strength at axial failure. To achieve this goal, a simple expression based on the linear trend observed in Hassan [7] for NEES joints and for previous joint tests (with no slab and more cycles per drift level) that experienced axial failure can be formed as:

For NEES joints:

$$\left(\frac{\Delta}{L}\right)_{axial} = 0.15 - 0.27\left(\frac{P}{f_c^{'} A_j}\right) \tag{8.a}$$

For previous joint tests:

$$\left(\frac{\Delta}{L}\right)_{axial} = 0.11 - 0.28\left(\frac{P}{f_c^{'} A_j}\right) \tag{8.b}$$

Equation 8 is a generic empirical relation that can be used for preliminary purposes unless more test data is available to confirm it.

Another empirical expression can be developed based on shear friction influence parameters. Figure 8 shows the relationship between drift ratio at axial failure and the axial failure load normalized by beam bottom reinforcement strength (acting as shear friction reinforcement) and the critical angle of inclination of the crack, a key parameter in beam-column joint shear and axial capacity. The figure suggests an inverse proportionality reflected by a power based relationship that can be fitted directly relating drift ratio and normalized axial load as:

$$\left(\frac{\Delta}{L}\right)_{Axial} = 0.057\left(\frac{P.\tan\theta}{A_{sb} f_{yb}}\right)^{-0.5} \tag{9}$$

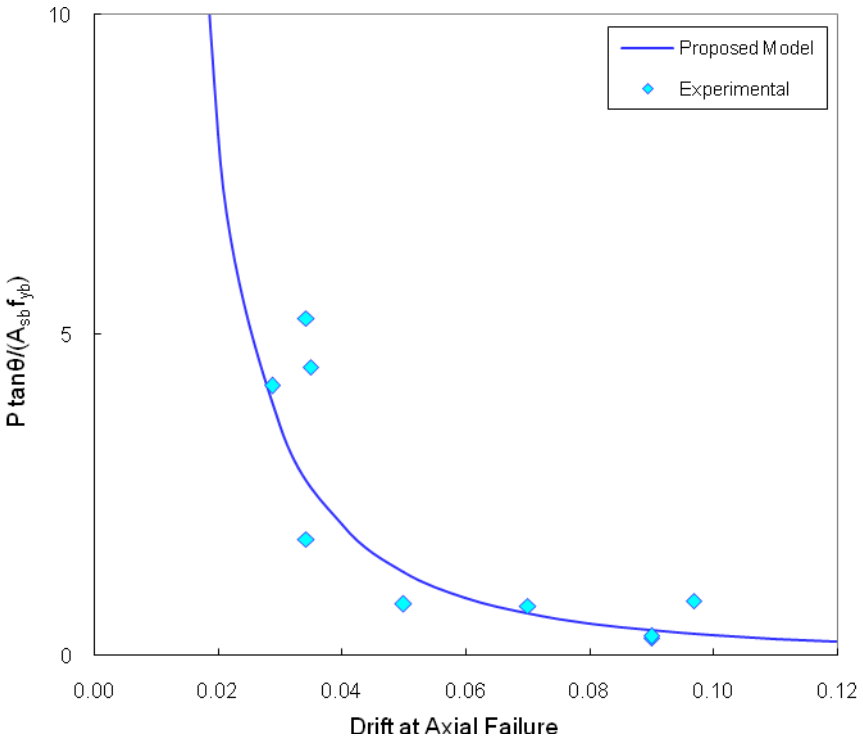

Figure 8 Proposed empirical model (Eq. 9) for drift capacity at axial failure

It was worthy also investigating the influence of other important parameters such as the concrete strength, joint effective area and column longitudinal reinforcement strength. These factors are common in axial capacity studies of columns. The results of this investigation presented in Hassan [7] suggested weak sensitivity of the axial failure model to these parameters.

This above discussion suggests the appropriateness of the empirical expression (Eq. 9) for quick estimation of drift capacity at joint axial failure. It is important to notice that this expression is based on a rather small joint axial failure database. Thus, more joint axial failure tests are needed to further verify this relation. In addition, it is worth mentioning that this expression is suitable for J-Failure joints with any axial load ratio, BJ-Failure joints with small axial load ratio, and BJ-Failure with high axial load ratio when the flexural capacity of the beam is close to the direct J-Failure strut-and-tie model capacity. The case of high axial load on a joint in a subassembly where the beam flexural capacity is much smaller than the direct J-failure capacity is excluded from the application of this model for reasons mentioned earlier.

5 PROPOSED MODELS EVALUATION

Figure 9 presents the correlation of the experimental drift capacity at axial failure to the calculated one using the shear-friction model for axial capacity (Eq. 3). The average test to model drift ratio is 1.00 and the COV is 0.27. It is also worth mentioning that residual shear capacity at axial failure is based on the NEES joint results; which led to the drift for other tests loaded with greater number of displacement cycles to be overestimated by the model.

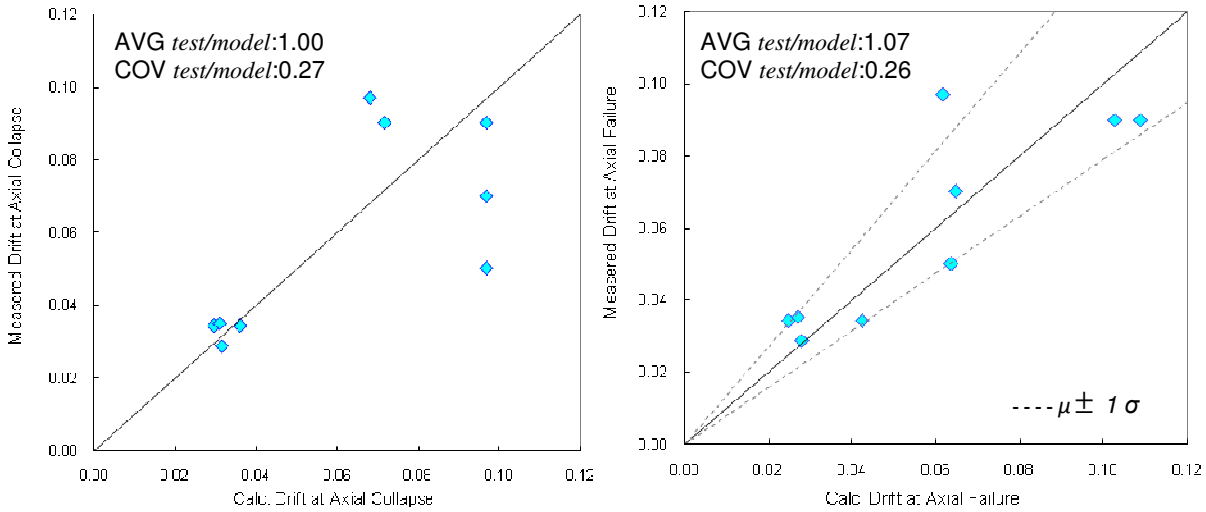

Figure 9 Correlation of the proposed axial capacity models to test results

The empirical axial capacity model proposed by Eq. 9 is evaluated against test results in Fig. 9. The ratio of test-to-model drift capacity was mean of 1.07 and COV of 0.26. Note that the calculated drift for specimen U-J-1 is underestimated by about 43%. During the U-J-1 test, the axial load dropped accidently after onset of shear failure. It is plausible that the drift ratio would have been decreased had the axial load remained high.

6 CONCLUSIONS

- An inverse proportionality between axial load and maximum drift reached before axial failure is evident for joints failing in the J-Failure mode. Joints with very high axial loads (perhaps larger than $0.45f_c'A_j$) experiencing BJ-Failure mode may benefit from higher axial load, such that they do not follow the aforementioned inverse relation.
- Although not isolated as an independent variable in this study, joints undergoing more rigorous loading history (for example, more cycles) generally had smaller drift at axial failure.
- The main resisting mechanism that supports axial loads in a shear damaged joints is believed to be shear friction on the previously damaged shear failure plane. The buckling capacity of column reinforcement is believed to be a secondary mechanism to shear friction mechanism, which is triggered upon shear friction failure.
- Unlike some cases of column axial failure, joint axial failure does not immediately follow joint shear failure. The ratio of drift at axial failure to drift at shear failure ranged from 2.5 to 3.3 for high axial loads, and from 3 to 5.5 for low axial load.
- An "axial failure safe zone" was identified based on the current and previous tests with and without axial failure. Joint axial failure was not observed for drift ratio demand below 2.5% - 3%. For drift ratios higher than 2.5% - 3%, axial failure was observed especially with increasing drift, axial load, or both.
- Joint axial capacity models were proposed based on the shear friction concept. The models correlated well with available data, but the data set was relatively small, such that additional model calibration is warranted.

ACKNOWLEDGEMENT

Financial assistance provided by U.S. National Science Foundation (NSF) award #0618804 through George E. Brown Jr. Network for Earthquake Engineering Simulation (NEES) and the Egyptian Department of Education award #2005292 through Building National Research Center is greatly appreciated.

REFERENCES

[1] Antonopoulos, C.P., and Triantafillou, T.C., Experimental Investigation of FRP Strengthened RC Beam-Column Joints, *ACSE Journal of Composites for Construction,* V.7, No. 1, pp 39-49, 2003.

[2] Clyde, C., Pantelides C. and Reaveley L., Performance-Based Evaluation of Exterior Reinforced Concrete Building Joints for Seismic Excitation. *PEER Report 2000-5, Pacific Earthquake Engineering Research Center (PEER)*, University of California, Berkeley, CA, July 2000.

[3] Elwood, K.J., and Moehle, J.P., Shake Table Tests and Analytical Studies on the Gravity Load Collapse of Reinforced Concrete Frames. *PEER Report 2003-01*, *Pacific Earthquake Engineering Research Center (PEER),* University of California, Berkeley, 2003.

[4] Engindeniz, M., Repair and Strengthening of Pre-1970 Reinforced Concrete Corner Beam-Column Joints Using CFRP Composites, *PhD Thesis, Civil and Environmental Engineering Department, Georgia Institute of Technology*, August 2008.

[5] Hanson N. W., and Connor, H. W., Seismic Resistance of Reinforced Concrete Beam Column Joints. *Journal of the Structural Division, Proceedings of the American Society of Civil Engineers*, Vol. 93, No. ST5, pp. 533-560, October 1967.

[6] Hanson N. W., and Connor, H. W., Tests of Reinforced Concrete Beam-Column Joints under Simulated Seismic Loading. *Research and Development Bulletin RD 012*, Portland Cement Association, 1972.

[7] Hassan, W. M., Analytical and Experimental Investigation of Seismic Vulnerability of Beam-Column Joints without Transverse Reinforcement in Concrete Buildings. *PhD Dissertation, University of California, Berkeley*, May 2011.

[8] Hassan, W. M. and Moehle, J. P., Experimental Assessment of Seismic Vulnerability of Corner Beam-Column Joints in Older Concrete Buildings. *Proceedings of the 15th World Conference of Earthquake Engineering*, Lisbon, Portugal, September, 2012.

[9] Hassan, W. M. and Moehle, J. P., A Cyclic Nonlinear Macro Model for Numerical Simulation of Beam-Column Joints in Existing Concrete Buildings. *Proceedings of the 15th World Conference of Earthquake Engineering*, Lisbon, Portugal, September, 2012.

[10] Hassan, W. M., Park, S., Lopez, R.R., Mosalam, K. M., and Moehle, J. P., Seismic Response of Older-Type Reinforced Concrete Corner Joints*, Proceedings of the 9th U.S. National and 10th Canadian Conference on Earthquake Engineering*, Toronto, Ontario, Canada, July 25-29, 2010.

[11] Hwang, S.J., Lee, H.J., Liao, T.F., Wang, K.C., and Tsai, H.H., Role of Hoops on Shear Strength of Reinforced Concrete Beam-Column Joints. *ACI Structural Journal*, V. 102, No. 3, pp. 445-453, 2005.

[12] Karayannis, C.G., Chalioris, C.E., and Sirkelis, G.M., Local Retrofit of Exterior RC Beam-Column Joints Using Thin RC Jackets: An Experimental Study. *Earthquake Engineering and Structural Dynamics*, V. 37, pp. 727-746, 2008.

[13] National Information Service for Earthquake Engineering (NISEE), *Pacific Earthquake Engineering Center*, University of California, Berkeley, 2010.

[14] Pagni, C.A., Modeling of Structural Damage of Older Reinforced Concrete Components. *M.Sc. Thesis, University of Washington*, 2003

[15] Pantelides, C., Hansen, J. and Reaveley, L., Assessment of Reinforced Concrete Building Exterior Joints With Substandard Details. *Technical Report PEER 2002-18, Pacific Earthquake Engineering Research Center (PEER)*, University of California, Berkeley, CA, May 2002.

[16] Park, S., Experimental and Analytical Studies on Old Reinforced Concrete Buildings with Seismically Vulnerable Beam-Column Joints. *PhD Dissertation, University of California, Berkeley*, December 2010.

[17] Priestley, M.J.N. and Hart, G., Royal Palm Resort, Guam, Seismic Behavior of As-Built and As-Designed Corner Joints. *SEQAD Consulting Engineers*, Solana Beach, CA, 1994.

[18] Tsonos, A. G., Effectiveness of CFRP-Jackets and RC-Jackets in Post-Earthquake and Pre-Earthquake Retrofitting of Beam–Column Sub-assemblages, *Engineering Structures,* Vol.30, pp. 777-793, 2008.

[19] Uzumeri, S. M., Strength and Ductility of Cast-in-Place Beam Column Joints. *Reinforced Concrete Structures in Seismic Zones, SP-53, Hawkins, N. M., ed., American Concrete Institute*, Detroit, Michigan, pp. 293-350, 1977.

[20] Wong, H.F., Shear Strength and Seismic Performance of Non-Seismically Designed Reinforced Concrete Beam-Column Joints. *PhD Dissertation, Department of Civil Engineering, The Hong Kong University of Science and Technology,* August 2005.